

## ANISOTROPY IN THE DISTRIBUTION OF SATELLITE GALAXY ORBITS

ALEXANDER KNEBE<sup>1</sup>, STUART P.D. GILL<sup>1</sup>, BRAD K. GIBSON<sup>1</sup>, GERAINT F. LEWIS<sup>2</sup>, RODRIGO A. IBATA<sup>3</sup>,  
AND MICHAEL A. DOPITA<sup>4</sup>*Draft version November 15, 2018*

## ABSTRACT

Nearby clusters such as Virgo and Coma possess galaxy distributions which tend to be aligned with the principal axis of the cluster itself. This has also been confirmed by a recent statistical analysis of some 300 Abell clusters where the effect has been linked to the dynamical state of the cluster. Moreover, the orbits of satellite galaxies in galactic systems like our own Milky Way also demonstrate a high degree of anisotropy – the so-called Holmberg effect, the origin of which has been the subject of debate for more than 30 years. This study presents the analysis of cosmological simulations focusing on the orbits of satellite galaxies within dark matter halos. The apocentres of the orbits of these satellites are preferentially found within a cone of opening angle  $\sim 40^\circ$  around the major axis of the host halo, in accordance with the observed anisotropy found in galaxy clusters. We do, however, note that a link to the dynamical age of the cluster is not well established as both our oldest dark matter halos do show a clear anisotropy signal. Further analysis connects this distribution to the infall pattern of satellites along the filaments: the orbits are determined rather by the environment of the host halo than some "dynamical selection" during their life within the host's virial radius.

*Subject headings:* galaxies: formation — cosmology: theory — methods: numerical

## 1. INTRODUCTION

Observations of the distribution of bright elliptical galaxies within the Virgo galaxy cluster show a remarkable collinear arrangement (West & Blakeslee 2000). Moreover, this axis also appears to be part of a filamentary bridge connecting Virgo and the rich cluster Abell 1367. This phenomenon has already been recognized (Arp 1968; Bingegeli, Tammann & Sandage 1987) but only with accurate measurements of distance did it become possible to discriminate between this being a genuine three-dimensional structure or merely a chance alignment of galaxies. West & Blakeslee (2000) based their distances upon the surface brightness fluctuations method (cf. Blakeslee, Ajhar & Tonry 1999 for a recent review), concluding that not only were the brightest cluster members distributed anisotropically over the cluster, but the distribution of dwarf ellipticals was elongated in the same direction (Binggelli 1999). Plionis et al. (2003) investigated this substructure-cluster correlation statistically using 303 Abell clusters. They affirm that there is indeed such a signal and also that this signal is related to the dynamical state (and the environment) of the cluster.

Moreover, even on smaller scales – in galactic systems – there are clear observational indications that the distribution of the orbits of satellite galaxies is biased towards the galactic pole (Holmberg 1969) giving an anisotropic distribution. Zaritsky et al. (1997) found that satellites of (isolated) disk galaxies are scattered asymmetrically about the parent galaxy and aligned preferentially with the disk minor axis. At first this signal was only prominent for distances out to  $\sim 50$  kpc from the host (Holmberg 1969), but an analysis based on a much larger sample (cf. Zaritsky et al. 1993) of satellites extends it to 200 kpc (Zaritsky et al. 1997). This result is confirmed by a study of the satellites orbiting M31 (Hartwick 2000;

Grebel, Kolatt & Brandner 1999). In addition, for the one galaxy where individual satellite orbits are known, the Milky Way, there is also evidence that the orbits are preferentially polar (Zaritsky & Gonzalez 1999). This is derived from information based upon the alignment of satellites on the sky (Kunkel & Demers 1976; Lynden-Bell 1982), the orientation of the Magellanic Stream (Mathewson, Clearly & Murray 1974), the three-dimensional distribution of satellites (Majewski 1994; Hartwick 1996), and their actual velocities (Scholz & Irwin 1994).

All these observations clearly indicate that on scales spanning from galaxy clusters down to galaxies there is a signal indicating a correlation between the alignment of substructure and the shape of the gravitational potential this substructure moves in. However, the source of this alignment of satellites has been debated for a number of years, with two potential solutions suggested to explain this puzzling arrangement. If the distribution of infalling satellites is initially spherical, then dynamical selection may preferentially destroy or suppress the star-formation in those on more equatorial orbits<sup>5</sup>. For instance, Peñarubbia, Kroupa & Boily (2002) have argued that in flattened dark matter halos, the timescale for dynamical friction is substantially longer for satellites that are on polar orbits. Alternatively, the present non-isotropic distribution of satellite systems may reflect the fact that it has always been non-isotropic, with the satellites being accreted along preferred directions. These hypotheses can be tested in numerical simulations of structure formation. However, in previous attempts to decipher this signal from cosmological  $N$ -body simulations there still remains a certain amount of uncertainty (Zaritsky et al. 1997). The first fully self-consistent simulations targeting the subject were performed by Tormen (1997). They though lacked resolution in time, space and mass to perform a detailed analysis of the satel-

<sup>1</sup>Centre for Astrophysics & Supercomputing, Swinburne University, Mail#31, PO Box 218, Hawthorn, VIC 3122, Australia.

<sup>2</sup>Institute of Astronomy, School of Physics, A29, University of Sydney, NSW 2006, Australia

<sup>3</sup>Observatoire de Strasbourg, 11, Rue de l'Université, F-6700, Strasbourg, France

<sup>4</sup>Research School of Astronomy and Astrophysics, Australian National University, Weston Creek Post Office, ACT 2611, Australia

<sup>5</sup>With *equatorial* we mean "perpendicular to the major axis"

lite population for differing environments, and hence more refined simulations are required. Tormen (1997) could not follow the satellite distribution within the host's virial radius but rather tracked all progenitors prior to accretion. This allowed him to analyze the infall pattern rather than the orbital evolution of the satellites. The aim of this study is to investigate this subject with the latest state-of-the-art high-resolution  $N$ -body-simulations. We focus upon a detailed analysis of the temporal and spatial properties of satellite galaxies residing within host galaxy clusters that formed fully self-consistently within a cosmological framework.

## 2. THE SIMULATIONS

There is mounting evidence that, despite its problems, the Cold Dark Matter structure formation scenario provides the most accurate description of our Universe. Observations point towards the standard  $\Lambda$ CDM according to which the universe is comprised of about 28% dark matter, 68% dark energy, and luminous baryonic matter (i.e. galaxies, stars, gas, and dust) at a mere 4% level (cf. Spergel et al. 2003). This so-called "concordance model" induces hierarchical structure formation in which small objects form first and subsequently merge to form larger objects.

The analysis presented in this study is based upon a suite of eight high-resolution  $N$ -body simulations within the  $\Lambda$ CDM concordance cosmology. They were carried out using the publicly available adaptive mesh refinement code MLAPM (Knebe, Green & Binney 2001). MLAPM reaches high force resolution by refining all high-density regions with an automated refinement algorithm. The refinements are recursive: the refined regions can also be refined, each subsequent refinement having cells that are half the size of the cells in the previous level. This creates an hierarchy of refinement meshes of different resolutions covering regions of interest. The refinement is done cell-by-cell (individual cells can be refined or de-refined) and meshes are not constrained to have a rectangular (or any other) shape. The criterion for (de-)refining a cell is simply the number of particles within that cell and a detailed study of the appropriate choice for this number as well as more details about the particulars of the code can be found elsewhere (Knebe, Green & Binney, 2001).

Each run focuses on the formation and evolution of one particular dark matter halo containing of order greater one million particles. The force resolution reached by MLAPM in the high-density regions is  $2h^{-1}$  kpc corresponding to roughly 0.25% of the host's virial radii  $R_{\text{vir}}$ . Following Lacey & Cole (1994) we define the formation redshift  $z_{\text{form}}$  as the time when the halo contains half of its mass today. The host halos were carefully chosen to sample a variety of different triaxialities and merger histories as summarized in Table 1. The virial radii given in that Table correspond to the point where the density of the host (measured in terms of the cosmological background density  $\rho_b$ ) drops below  $\Delta_{\text{vir}} = 340$  with  $M_{\text{vir}}$  being the mass enclosed by that sphere. All satellite galaxies orbiting in and around the host halo are identified using the MLAPM-based halo finder described in a companion paper (Gill, Knebe & Gibson 2004). This new halo finder is based upon the MLAPM grid structure and works at the same resolution level as the  $N$ -body code itself thus assuring not to miss or include any objects not resolved in the actual simulation. The satellites are then individually traced from  $z_{\text{form}}$  onwards until redshift  $z = 0$ . The mass spectrum of those satellites accounted for in the following analysis can be described by a declining power-law  $dn/dM \propto M^{-\alpha}$  with  $\alpha \approx 1.7 - 1.9$  in

the range from  $2 \times 10^{10} h^{-1} M_{\odot}$  (applied mass-cut corresponding to 100 particles and explaining the rather 'low' number for  $N_{\text{sat}}(< r_{\text{vir}})$  in Table 1) up to  $\sim 10^{13} h^{-1} M_{\odot}$ . The total fraction of mass locked up in satellites never exceeds  $\leq 15\%$  though.

The high temporal sampling of the outputs (i.e.  $\Delta t \approx 0.2$  Gyrs) allows us to accurately measure the orbital parameters of the satellite galaxies and a detailed analysis of their disruption and survival history will be presented elsewhere (Gill, Knebe & Gibson 2004). Gill et al. show that the distribution of orbital eccentricities of the satellite population peaks about the value  $\epsilon \approx 0.6$  where  $\epsilon = 1 - p/a$  is defined using the last pericenter  $p$  and apocenter  $a$  of its orbit. The pericenter distribution itself peaks about 35% of  $R_{\text{vir}}$  for all host halos and most of the satellites (i.e. more than 75%) had had one full orbit with the maximum number of orbits found to be 3–5 depending on the host halo. The angular momentum vector of the satellite  $\vec{L}_{\text{sat}}^{\text{apo}} = \vec{R}_{\text{sat}}^{\text{apo}} \times \vec{V}_{\text{sat}}^{\text{apo}}$  was calculated at its last apocenter passage  $\vec{R}_{\text{sat}}^{\text{apo}}$ .

In order to probe the alignment with the shape and orientation of the host halo we calculated the eigenvectors  $\vec{E}_{1,2,3}$  (with  $\vec{E}_1$  being the major axis) of its inertia tensor using only the "core" region as defined by the 6<sup>th</sup> refinement level in MLAPM, i.e. the boundary of this refinement level is an isodensity contour. According to the refinement criterion adopted in the simulations the 6<sup>th</sup> level surrounds material about 3000 times denser than  $\rho_b$  or in other words 9 times denser than the material at the virial radius. The host halos are well described by the density profiles advocated by Navarro, Frenk & White (1997) with concentration in the range  $c = 5 - 7$ . Therefore, a density of roughly  $9 \times \rho(r_{\text{vir}})$  corresponds to about the half-mass radius of the host. The eigenvectors now define the orientation of the host halo and the coordinate system used to measure the orbits of the satellites, respectively. Moreover, its eigenvalues  $a > b > c$  can be used to construct the triaxiality parameter  $T = (a^2 - b^2)/(a^2 - c^2)$  (Franx, Illingworth & Zeeuw 1991) presented in Table 1, too.

The left panel of Fig. 1 presents the (normalized) distribution of angles between  $\vec{R}_{\text{sat}}^{\text{apo}}$  and  $\vec{E}_{1,\text{host}}$ . This graph shows that there is a clear trend in at least six of the eight halos for the two vectors to be aligned (the distribution peaks at  $0^\circ$  and  $180^\circ$ , respectively) meaning that the orbits of the satellites are preferentially found along the major axis of the host. The right panel of Fig. 1 shows the (normalized) distribution of angles between the angular momentum vector  $\vec{L}_{\text{sat}}^{\text{apo}}$  of the satellite at its last apocenter and  $\vec{E}_{1,\text{host}}$ , clearly revealing evidence for these two vectors to be parallel (distribution peaks at  $90^\circ$ ). We like to stress that only satellite galaxies that at least had one or more complete orbits were taken into account in Fig. 1; the figure is *not* based upon the infall pattern of satellites as investigated by, for instance, Tormen (1997). We also need to stress that the distributions presented in that Figure are normalized, i.e. they are corrected for the bias introduced by plotting them as a function of the angle  $\theta$  rather than  $\cos\theta$ . The data is binned equally spaced in angle ranging from  $0^\circ$  to  $180^\circ$ , and therefore the area probed on the sphere varies with  $\theta$ . Therefore the distribution needed to be normalized by the the respective area  $A$  specified by the actual range of angles  $[\theta - \Delta\theta/2, \theta + \Delta\theta/2]$ . This area is proportional to  $A \propto \cos(\theta - \Delta\theta/2) - \cos(\theta + \Delta\theta/2)$ .

## 3. CONCLUSIONS AND DISCUSSION

There are two possible scenarios that explain the substructure-cluster alignment found in observations of galaxy clusters (Plionis et al. 2003; West & Blakeslee 2000) and the

TABLE 1  
SUMMARY OF THE EIGHT HOST DARK MATTER HALOS.

Halo	$R_{\text{vir}}[h^{-1} \text{ kpc}]$	$v_{\text{circ}}^{\text{max}}[\text{ km s}^{-1}]$	$M_{\text{vir}}[10^{14}h^{-1} M_{\odot}]$	$z_{\text{form}}$	age [Gyr]	$N_{\text{sat}}(< r_{\text{vir}})$	$T$
# 1	1349	1125	2.87	1.16	8.30	158	0.67
# 2	1069	894	1.42	0.96	7.55	63	0.87
# 3	1081	875	1.48	0.87	7.16	87	0.83
# 4	980	805	1.10	0.85	7.07	57	0.77
# 5	1356	1119	2.91	0.65	6.01	175	0.65
# 6	1055	833	1.37	0.65	6.01	85	0.92
# 7	1014	800	1.21	0.43	4.52	59	0.89
# 8	1384	1041	3.08	0.30	3.42	251	0.90

analysis of  $N$ -body-simulations presented in this study. Either some dynamical process can be held responsible, meaning that initially the orbits were randomly distributed and only some satellites survive to give rise to the observed correlation in Fig. 1, or alternatively, their orbital parameters are imprinted upon them at the time they enter the host halo as already pointed out by Tormen (1997).

“Dynamical destruction”, whereby satellites on more equatorial orbits suffer more tidal disruption, can be rejected because a comparable (although not as pronounced) alignment signal is found when restricting the analysis to those satellites that are in fact disrupted: We placed mass-less tracer particles at the last centre of the satellites before they were classified “disrupted”. These “disrupted systems” are presented as the thin lines in Fig. 1.

We therefore conclude that it must be the initial distribution of the satellite systems that is responsible for the present day alignment. For example, galaxies are “funneling along the filaments” (Kitzbichler & Saurer 2003) which has also been confirmed by X-ray observations of the spatial distribution of substructure in galaxy clusters (West, Jones & Forman 1995) and biases the types of possible orbits. It would now be reassuring to confirm a link between the host halo shape and the surrounding environment, i.e. are the filaments that feed the halo with material preferentially angled with respect to the orientation of the host halo? When projecting the positions of the satellites onto a sphere at the time they enter the virial radius of the host it is clear that they are not randomly distributed; they cluster in directions linked to the filamentary structure surrounding the host halo, as found before observationally (e.g. West & Blakeslee 2003; Plionis & Basilikos 2002, and references therein) and in  $N$ -body-simulations (e.g. Faltenbacher 2002; Hatton & Ninin 2001; Onuora & Thomas 2000; Colberg et al. 1999; Splinter et al. 1997; Tormen 1997). Tormen (1997) already pointed out that there is a strong alignment between the distribution of infalling satellite galaxies and the shape of the dark matter host. However, Tormen’s simulations did not have the spatial and mass resolution to investigate the orbits of satellites *within* the host halo. We are, for the first time, tracing extremely well-resolved dynamics of the satellites within the dark matter hosts confirming that the alignment for both, disrupted and surviving, satellites is maintained for several orbital periods. Fig. 2 now presents a visual impression of the trajectories of all surviving satellites identified at formation time of host halo #3 until redshift  $z = 0$ , qualitatively supporting the scenario that these orbits

are linked to the filamentary structure which will leave its imprint in observed anisotropy.

Plionis et al. (2003) also established a link between the alignment and the dynamical age of the clusters. Our simulations though show that this finding can not be generalized: both our oldest halos, in which the satellites had as many as 4–5 orbits, do show the correlation signal. We do not observe a trend for a “randomization” of the orbits in older halos. The satellites actually preserve the alignment with the host they had when they first fell into the cluster.

In Section 1 we showed that the (observational) substructure-alignment signal spans from galaxy clusters down to galactic scales. Our results are mostly applicable to the former, and any extrapolation to smaller scales has to be handled with care. In the case for galaxies, for instance, the interaction between the galactic disk and the incoming satellite could enhance destruction in the galaxy plane, i.e. satellite on prograde orbits decay faster than the ones on retrograde (or polar) orbits due to orbital resonances between the disk and the satellites (Peñarubia, Kroupa & Boily 2002). Based on theoretical and numerical studies (cf. Lacey & Cole 1993 and Moore et al. 1999) it should be possible to re-scale our simulations to a Milky Way sized object by requiring that the maximum of the circular velocity curves of our halos equals  $220 \text{ km s}^{-1}$ . The scaling factor lies in the range of about 4–5 (cf.  $v_{\text{circ}}^{\text{max}}$  values in Table 1) and hence our “rescaled dark matter halos” would correspond to the ones in the observational data with virial radii in the range  $260\text{--}295h^{-1} \text{ kpc}$ . This scaling factor in length entails a scaling in mass of 64–125 (simply the length scale to the power of three). This brings the mass of our galaxy clusters down to  $\sim 10^{12}h^{-1} M_{\odot}$  which agrees with the dark matter mass inferred for our Milky Way (Freeman 1996). More problematic, however, are the ages of our systems: our halos are only  $\leq 8.3$  Gyrs old opposed to 12 Gyrs for the Milky Way. Satellites in the Milky Way had the chance to complete nearly twice as many orbits leaving more space for an explanation based upon the dynamical destruction scenario.

When re-scaling our data, putting aside the age issue, and trying to explain the Holmberg effect, another uncertainty comes into play: the orientation of the stellar disk. In a triaxial potential there are in general stable closed orbits about both the major and the minor axis (e.g., Binney & Tremaine 1987). So, in principal the disk plane could either be perpendicular to the major or perpendicular to the minor axis. Under the assumption it lies perpendicular to the major axis of the dark matter halo

the satellites in our simulations will be on polar orbits. There are indications that this configuration results in the most stable disk configuration within a triaxial halo (Hayashi et al. 2003). Moreover, even though there are clear indications that the angular momentum of the dark matter is well aligned with the minor axis of the halo (e.g. Warren et al. 1992), van den Bosch et al. (2002) showed that the angular momentum of the baryonic component (i.e. gas) not necessarily follows that of the dark matter distribution. They found an average misalignment between  $\vec{L}_{\text{gas}}$  and  $\vec{L}_{\text{DM}}$  of the order of  $40^\circ$  in their numerical simulations. Hence the orientation of the galactic disk with respects to the dark matter halo is not well determined. Turning to observations does not resolve this question, with studies of polar rings indicating strongly oblate halos

(i.e. Iodice et al. 2003), while others suggest dark matter halos are more spherical, or even oblate (Olling & Merrifield 2000; Ibata et al. 2001). The situation is not at all clear, but the assumption that disks are perpendicular to the major axis (which is in agreement with results presented by Hayashi et al. 2003) would provide an explanation for the Holmberg effect, even though this is a very speculative interpretation.

The simulations presented in this paper were carried out on the Beowulf cluster at the Centre for Astrophysics & Supercomputing, Swinburne University. The support of the Australian Research Council and the Swinburne Research Development Grants Scheme is gratefully acknowledged. GFL thanks Suede for “Introducing the band”.

#### REFERENCES

- Binney J., Tremaine S., 1987, *Galactic Dynamics* (Princeton: Princeton University Press)
- Bullock, J., Kravtsov, A., Weinberg, D. 2000, ApJ 539, 517
- Colberg J.M., White S.D.M., Jenkins A., Pearce F.R., 1999, MNRAS, 308, 593
- Cote P. et al. , 2001, ApJ, 559, 828
- Dalal N., Kochanek C.S., 2002, ApJ, 572, 25
- Evans N.W., Witt H.J., 2003, *astro-ph/0212013*
- Franx M., Illingworth G., de Zeeuw T., 1991, ApJ, 383,112
- Freeman K.C., 1996, in ASP Conf. Proc. 92, Formation of the Galactic Halo - Inside and Out, ed. H. Morrison & A. Sarajedini (San Francisco: ASP), p.3
- Gill S., Knebe A., Gibson B.K., 2004, in preparation
- Grebel E.K., Kolatt T., Brandner W., 1999, in *The stellar content of the Local Group*, IAU 192, eds. P. Whitelock & R. Cannon, San Francisco: ASP Conf. Series
- Hayashi E. et al. , 2003, in preparation
- Holmberg E., 1969, Ark. Astron., 5, 305
- Hatton S., Ninin S., 2001, MNRAS, 322, 576
- Ibata R., Lewis G. F., Irwin M., Totten E., & Quinn T., 2001, ApJ, 551, 294
- Iodice E., Arnaboldi M., Bournaud F., Combes F., Sparke L. S., van Driel W., & Capaccioli M. 2003, ApJ, 585, 730
- Kitzbichler M.G., Saurer W., 2003, ApJ, 590, L9
- Klypin A.A., Kravtsov A.V., Valenzuela O., Prada F., 1999, ApJ, 522, 82
- Knebe A., Green A., Binney J.J., 2001, MNRAS, 325, 845
- Kunkel W.E., Demers S., 1976, Roy. Green. Obs. Bull., 182, 241
- Lacey C., Cole S., 1993, MNRAS, 262, 627
- Lacey C., Cole S., 1994, MNRAS, 271, 676
- Lynden-Bell D., 1982, Observatory, 102, 202
- Majewski S.R., 1994, ApJ, 431, L17
- Matthewson D.S., Clearly M.N., Murray J.D., 1974, ApJ, 190, 291
- Moore B., Ghigna S., Governato F., Lake G., Quinn T., Stadel J., Tozzi P., 1999, ApJ, 524, L19
- Olling, R. P. & Merrifield, M. R. 2000, MNRAS, 311, 361
- Peñarubbia, J., Kroupa, P., Boily, C. 2002, MNRAS, 333, 779
- Plionis M., Basilikos S., 2002, MNRAS, 329, L47
- Scholz R.-D., Irwin M.J., 1994, in IAU 161, *Wide Field Imaging*, eds. H.T. MacGillivray
- Schechter P. L. & Wambsgans J. 2002, ApJ, 580, 685
- Spergel D.N., Steinhardt P.J., 2000, Phys. Rev. Lett., **84**, 3760
- Somerville, R. 2002, ApJ, 572, 23
- Tormen G., 1997, MNRAS, 290, 411
- Tully, B., Somerville, R., Trentham, N., Verheijen, M. 2002, ApJ, 569, 573
- Warren M.S., Quinn P.J., Salmon J.K., Zurek W.H., 1992, ApJ, 399, 405
- West M.J., Jones C., Forman W., ApJ, 451, L5
- West M.J., Blakeslee J.P., 2000, ApJ, 543, L27
- Zaritsky D., Smith R., Frenk C.S., White S.D.M., 1993, ApJ, 405, 464
- Zaritsky D., Smith R., Frenk C.S., White S.D.M., 1997, ApJ, 478, L53
- Zaritsky D., Gonzalez A.H., 1999, PASP, 111, 1508

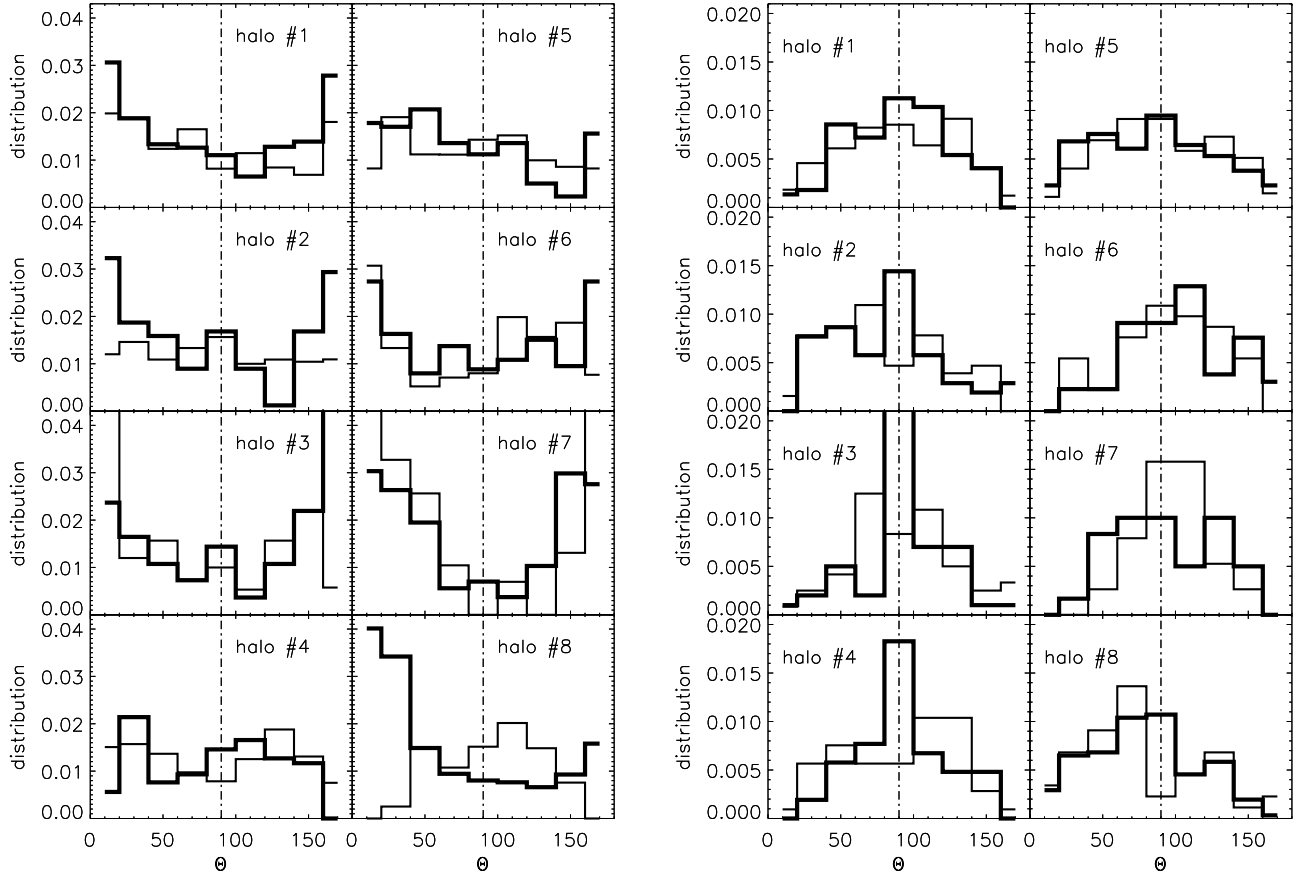


FIG. 1.— The left panel shows the (normalized) distribution of angles between position vector  $\vec{R}_{\text{sat}}^{\text{apo}}$  of the satellites measured at the last apocentre and the major axis  $\vec{E}_{1,\text{host}}$  of the halo.  $\theta$  values of  $0^\circ$  and  $180^\circ$  indicate alignment with the the principal axis of the host. The right panel shows the (normalized) distribution of angles between angular momentum vector  $\vec{L}_{\text{sat}}^{\text{apo}}$  of satellites measured at the last apocentre and the major axis  $\vec{E}_{1,\text{host}}$  of the halo. A  $\theta$  value of  $90^\circ$  means that the orbital plane of the satellite contains the major axis of the host where  $\theta$  of  $0^\circ$  and  $180^\circ$  would require for the plane to be perpendicular to the host's principal axis. The thin histograms are for disrupted satellites. In both cases only satellites more massive than  $2 \times 10^{10} h^{-1} M_\odot$  (100 particles) that had one full orbit were taken into account.



FIG. 2.— Orbits of all satellite galaxies identified at formation time (dark) to redshift  $z = 0$  (light). The left panel shows how the host halo fits into the surrounding large-scale structure presented at formation time. The right panel zooms into the region marked in the left panel, this time not showing low-resolution particles. The shape (and position) of the underlying host halo at redshift  $z = 0$  is indicated by the best-fit ellipse to the grid used to calculate its triaxiality. The vertical line extending to top edge of panel indicates the principal axis of the host. With the assumptions presented in this paper, the pole of the host galaxy within the dark matter halo is aligned with this principle axis.

This figure "figure2.jpg" is available in "jpg" format from:

<http://arxiv.org/ps/astro-ph/0311202v1>